Theoretical and Experimental Multi-Sensor Signal Detection in Time Spreading Distortion Underwater Channels

Rami Rashid
ECE Dept., NJIT
Newark, NJ, United States
raa62@njit.edu

Erjian Zhang
ECE Dept., NJIT
Newark, NJ, United States
ez7@njit.edu

Ali Abdi
ECE Dept., NJIT
Newark, NJ, United States
ali.abdi@njit.edu

Zoi-Heleni Michalopoulou
Math. Sciences. Dept., NJIT
Newark, NJ, United States
michalop@njit.edu

***Abstract* — A signal in shallow water environments typically undergoes distortion caused by time spreading, which refers to receiving multiple copies of the signal at different times due to signal propagation through multiple paths. This distortion makes signal detection a challenging task. In this paper, we present a systematic framework for signal detection in time-spreading distortion underwater channels using multiple sensors. Using Monte Carlo simulations as well as experimental data collected at hydrophones, the performance of the detector is evaluated. Our results quantify the effect of the number of correlators per sensor on the detection performance, as well as the improvement obtained by using multiple sensors in time-spreading distortion underwater channels.**

Keywords—Time dispersion, Multipath channels, Underwater channels, Signal detection, Multiple sensors.

I. INTRODUCTION

The received signals in multipath underwater channels can be severely impacted by time-spreading distortion (TSD), especially in shallow water. The likelihood ratio test (LRT) detector for TSD channels using a single sensor is studied in [1-3] and is called the Replica Correlation Integration (RCI) detector. This detector can be used to detect signals collected by underwater scalar and vector sensors [4]. It can also be integrated into the MIMO sonar for multipath channels [5]. In this paper, we present a systematic and unified framework for signal modeling and detection in TSD underwater channels using multiple sensors (extension to joint detection and localization [6] is also possible).

In this work, single-sensor and then multi-sensor detector formulations are presented, followed by performance assessment using simulations, as well as experimental data collected using hydrophones.

II. LIKELIHOOD RATIO DETECTOR IN TSD CHANNELS

In this section, first we introduce proper notation and equations for signal, channel and noise, in order to derive the single-sensor LRT detector in TSD channels. Then we expand those to derive the multi-sensor LRT detector, which is suitable for TSD channels.

A. Single-Sensor Detector

We define two binary hypotheses H_0 and H_1, where H_0 is the noise-only hypothesis; H_1 represents the hypothesis in which the transmitted signal $s[i]$ propagates through the TSD channel $h[l]$ and is then corrupted by additive noise $v[i]$:

$$H_0 : \mathbf{r} = \mathbf{v}, \tag{1}$$

$$H_1 : \mathbf{r} = \mathbf{x} + \mathbf{v}. \tag{2}$$

In the above equations, $\mathbf{r}$ is a complex vector with N elements:

$$\mathbf{r} = [r[0]\ r[1]\ \cdots r[N-1]]^T, \tag{3}$$

where ^{T} is the transpose, $\mathbf{v}$ is the $N\times 1$ complex noise vector

$$\mathbf{v} = [v[0]\ v[1]\ \cdots v[N-1]]^T, \tag{4}$$

and $\mathbf{x}$ is an $N\times 1$ complex vector that represents the known deterministic signal $s[i]$ convolved with the TSD random channel function $h[l]$ with duration of T_h and M_h equally-spaced samples, where $M_h = T_h f_s$ and f_s is the sampling frequency. The convolution embedded in $\mathbf{x}$ can be written as

The work is supported in part by NSF, Grant IIP-1500123, and ONR, Grant N00014-20-1-2029.

$$\mathbf{x} = (a / M_h^{1/2})\mathbf{S}\mathbf{h}, \tag{5}$$

where a represents echo attenuation [2] and $\mathbf{h}$ is the following $M_h \times 1$ complex random TSD channel vector

$$\mathbf{h} = [h[0]\ h[1]\ \cdots h[M_h - 1]]^T, \tag{6}$$

with the following covariance matrix

$$\mathbf{C}_\mathbf{h} = E[\mathbf{h}\mathbf{h}^\dagger], \tag{7}$$

in which † represents the transpose conjugate and E is the mathematical expectation. Additionally, $\mathbf{S}$ in (5) is the $N \times M_h$ transmitted signal matrix given by [7]

$$\mathbf{S} = \begin{bmatrix} s[0] & 0 & \cdots & 0 \\ s[1] & s[0] & \cdots & 0 \\ \vdots & \vdots & \ddots & \vdots \\ s[N-1] & s[N-2] & \cdots & s[N-M_h] \end{bmatrix}, \tag{8}$$

where the l^{th} column can be represented by the following vector

$$\mathbf{s}_l = [s[0-l]\ s[1-l]\ \cdots s[N-1-l]]^T, \quad l = 0,1,...,M_h - 1, \tag{9}$$

in which $s[i] = 0$ for $i < 0$ and $i > N-1$.

To simplify the notation, we assume that the signals are approximately orthogonal [2], with this correlation

$$R_s[l,l'] = \sum_{i=0}^{N-1} s^*[i-l]s[i-l'] / N = \mathbf{s}_l^\dagger \mathbf{s}_{l'} / N \approx \delta[l'-l], \tag{10}$$

where * is the conjugate and $\delta[.]$ is the Kronecker delta function. Equation (10) results in $\mathbf{S}^\dagger\mathbf{S} \approx \mathcal{E}\,\mathbf{I}_{M_h}$ for large N, where $\mathcal{E} = \sum |s[i]|^2$ is signal energy and $\mathbf{I}_{M_h}$ is an $M_h \times M_h$ identity matrix. We also consider that the noise vector $\mathbf{v}$ has a zero mean complex white Gaussian distribution with variance σ_v^2.

The optimal Neyman-Pearson detector [8] for this TSD channel formulation using one sensor can be shown to have the following log LRT statistic and decides H_1 if

$$\Lambda(\mathbf{r}) = \mathbf{r}^\dagger \mathbf{C}_\mathbf{x}(\mathbf{C}_\mathbf{x} + \sigma_v^2 \mathbf{I}_N)^{-1}\mathbf{r} > \eta, \tag{11}$$

where η is the threshold and $\mathbf{C}_\mathbf{x}$ is $N \times N$ covariance matrix for $\mathbf{x}$

$$\mathbf{C}_\mathbf{x} = a^2 M_h^{-1}\mathbf{S}\mathbf{C}_\mathbf{h}\mathbf{S}^\dagger. \tag{12}$$

When the TSD channel vector $\mathbf{h}$ - that is independent of the noise vector $\mathbf{v}$ - has a zero mean complex white Gaussian distribution with variance σ_h^2, we obtain $\mathbf{C}_\mathbf{h} = \sigma_h^2 \mathbf{I}_{M_h}$, which simplifies the covariance matrix of $\mathbf{x}$ to

$$\begin{aligned} \mathbf{C}_\mathbf{x} &= a^2 M_h^{-1}\sigma_h^2 \mathbf{S}\mathbf{S}^\dagger \\ &= a^2 M_h^{-1}\sigma_h^2 \sum_{l=0}^{M_h-1} \mathbf{s}_l \mathbf{s}_l^\dagger. \end{aligned} \tag{13}$$

Using the matrix inversion lemma [8], together with $\mathbf{S}^\dagger\mathbf{S} \approx \mathcal{E}\,\mathbf{I}_{M_h}$ presented after (10), (11) simplifies to

$$\Lambda(\mathbf{r}) = g\mathbf{r}^\dagger \mathbf{S}\mathbf{S}^\dagger \mathbf{r} > \eta, \tag{14}$$

where $g = (\mathcal{E} + a^{-2} M_h \sigma_v^2 \sigma_h^{-2})^{-1}$. Furthermore, we can rewrite (14) using the summation expression for $\mathbf{S}\mathbf{S}^\dagger$ in (13) as follows

$$\Lambda(\mathbf{r}) = g\sum_{l=0}^{M_h-1} \left|\mathbf{s}_l^\dagger \mathbf{r}\right|^2 = g\sum_{l=0}^{M_h-1} \left|\sum_{i=0}^{N-1} s^*[i-l]r[i]\right|^2 > \eta. \tag{15}$$

The double summation in (15) agrees with (10) in [2], called the RCI detector.

B. Multi-Sensor Detector

Here we consider the same hypotheses as (1) and (2), where now $\mathbf{r}$, $\mathbf{v}$ and $\mathbf{x}$ are complex vectors of size $KN \times 1$, in which N is the number of the samples that are collected by each sensor and K is the number of sensors

$$\mathbf{r} = [\mathbf{r}^T[0]\ \mathbf{r}^T[1]\ \cdots \mathbf{r}^T[N-1]]^T, \tag{16}$$

$$\mathbf{r}[i] = [r_0[i]\ r_1[i]\ \cdots r_{K-1}[i]]^T, \quad i = 0,1,...,N-1, \tag{17}$$

where $r_k[i]$ represents the received signal at the i^{th} time index and by the k^{th} sensor, and $\mathbf{v}$ has the same structure as (16), given by

$$\mathbf{v} = [\mathbf{v}^T[0]\ \mathbf{v}^T[1]\ \cdots\ \mathbf{v}^T[N-1]]^T, \tag{18}$$

$$\mathbf{v}[i] = [v_0[i]\ v_1[i]\ \cdots\ v_{K-1}[i]]^T, \quad i = 0,1,..,N-1, \tag{19}$$

where $v_k[i]$ represents the noise at the i^{th} time index and the k^{th} sensor. The convolution embedded in $\mathbf{x}$ can be written according to (5), where $\mathbf{h}$ now is the $KM_h \times 1$ complex random TSD channel vector

$$\mathbf{h} = [\mathbf{h}^T[0]\ \mathbf{h}^T[1]\ \cdots \mathbf{h}^T[M_h - 1]]^T, \tag{20}$$

$$\mathbf{h}[l] = [h_0[l]\ h_1[l]\ \cdots h_{K-1}[l]]^T, \quad l = 0,1,..,M_h - 1, \tag{21}$$

in which $h_k[l]$ represents the TSD random channel function at

the l^{th} time index and measured at the k^{th} sensor. Furthermore, now $\mathbf{S}$ is the $KN \times KM_h$ matrix of the transmitted signal, given by

$$\mathbf{S} = \begin{bmatrix} s[0]\mathbf{I}_K & \mathbf{0} & \cdots & \mathbf{0} \\ s[1]\mathbf{I}_K & s[0]\mathbf{I}_K & \cdots & \mathbf{0} \\ \vdots & \vdots & \ddots & \vdots \\ s[N-1]\mathbf{I}_K & s[N-2]\mathbf{I}_K & \cdots & s[N-M_h]\mathbf{I}_K \end{bmatrix}, \quad (22)$$

with $\mathbf{I}$ and $\mathbf{0}$ being identity and zero matrices, respectively.

Considering a white Gaussian distribution with variance σ_v^2 for the noise vector $\mathbf{v}$, the multi-sensor log LRT statistic can be derived as follows and decides H_1 if

$$\Lambda(\mathbf{r}) = \mathbf{r}^\dagger \mathbf{C}_\mathbf{x} (\mathbf{C}_\mathbf{x} + \sigma_v^2 \mathbf{I}_{KN})^{-1} \mathbf{r} > \gamma, \quad (23)$$

where (23) is the optimal Neyman-Pearson multi-sensor detector [8] derived for our TSD channel formulation, γ is the threshold, and $\mathbf{C}_\mathbf{x}$ is the $\mathbf{x}$ $KN \times KN$ covariance matrix, with the same structure as (12). For temporally and spatially uncorrelated TSD channels we have $E[h_k[l]h_{k'}^*[l']] = \sigma_h^2 \delta[l'-l]\delta[k'-k]$ and $\mathbf{C}_\mathbf{h} = \sigma_h^2 \mathbf{I}_{KM_h}$, resulting in

$$\mathbf{C}_\mathbf{x} = a^2 M_h^{-1} \sigma_h^2 \mathbf{S}\mathbf{S}^\dagger. \quad (24)$$

Using the above result and the matrix inversion lemma together with the orthogonality property presented in (10) that leads to $\mathbf{S}^\dagger\mathbf{S} \approx \mathcal{E}\, \mathbf{I}_{KM_h}$, after several analytical steps (23) can be eventually simplified to

$$\Lambda(\mathbf{r}) = g \sum_{k=0}^{K-1} \sum_{l=0}^{M_h-1} \left| \sum_{i=0}^{N-1} s^*[i-l] r_k[i] \right|^2 > \gamma, \quad (25)$$

where $g = (\mathcal{E} + a^{-2} M_h \sigma_v^2 \sigma_h^{-2})^{-1}$. For $K = 1$, (25) simplifies to (15) for the single-sensor detector.

We notice that the multi-sensor detector in (25) is essentially an incoherent superposition of multiple correlators, where a correlator basically correlates the received signal from a sensor with an *l*-shifted copy of the transmitted signal. Simulation and measurement results using the multi-sensor detector in (25) are presented in the next section, as well as comparison with the single-sensor detector in (15).

III. Simulation Results

To implement the detector in (25) and study its performance, we simulate 10,000 signal receptions per sensor for K sensors. We use a linear frequency modulated (LFM) signal

$$s[i] = \exp(j2\pi W_0 (2T_0)^{-1} t^2)\big|_{t=i/f_s}, \quad (26)$$

where W_0 and T_0 are the signal bandwidth and duration, respectively, $-T_0/2 \le t \le T_0/2$, $i = 0,\ldots,N-1$, and $N = T_0 f_s$, with the parameter values chosen to be the same as in [1], i.e., $T_0 = 2$ s, $W_0 = 200$ Hz and $f_s = W_0$. The signal energy in g of (25) is $\mathcal{E} = N$, whereas the other parameters of g are chosen to be $a = 0.1$, $M_h = 10$, and $\sigma_v^2 = \sigma_h^2 = 1$. In simulations, essentially the LFM signal in (26) is convolved with $K = 5$ uncorrelated TSD channels of K sensors, each having M_h uncorrelated, zero-mean and unit-variance complex Gaussian samples. The additive noise terms are all spatio-temporally white, zero-mean and unit-variance complex Gaussians, independent of the TSD channels.

In Fig. 1, we plot the receiver operating characteristic (ROC) curves for multi- and single-sensor detectors, $K = 5$ and 1, respectively, using (25). The number of correlators M per sensor is chosen to be equal to, larger or smaller than the number of TSD channel samples $M_h = 10$, to study the effect of M. Additionally, to confirm the accuracy of Fig. 1, ROC curves are also generated using the matrix-form multi-sensor detector in (23), which completely agree with those generated using (25). This validates our derivations and results.

Upon inspecting Fig. 1, we observe that

- As the number sensors increases, the detection performance improves. One possible explanation is that the signal-to-noise ratio (SNR) increases as K increases (see TABLE I).

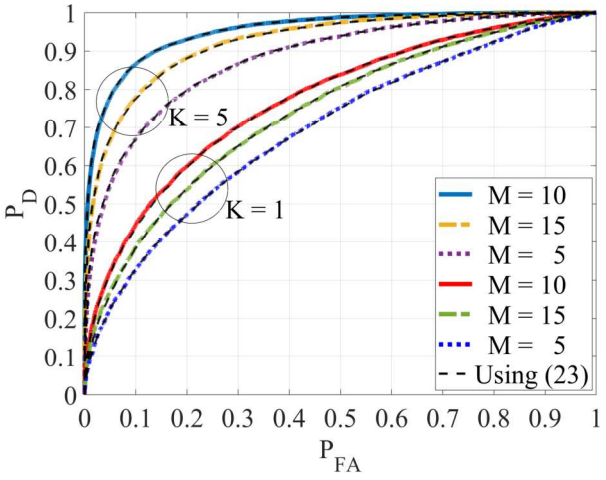

Fig. 1. Simulated ROC curves for the developed TSD channel multi-sensor detector in (25) (colored), and its matrix form in (23) (black dashed). We note the performance improvement as the number of sensors K increases from 1 to 5.

- When M is chosen to be equal to M_h, the best performan achieved for both single- and multi-sensor detectors.
- When M is chosen to be different from M_h, detection performance degrades for both single- and multi-sensor detectors. The performance loss appears to be less, when M is greater than M_h.

TABLE I. SNRs FOR THE ROC CURVES IN Fig. 1 (dB)

$M_h = 10$	$M = 5$	$M = 10$	$M = 15$
$K = 1$	9.9	12.9	13.8
$K = 5$	17	20	20.8

IV. EXPERIMENTAL RESULTS

In this section, we examine the performance of the proposed multi-sensor detector in (25) using experimental data collected by two hydrophones, A and B, in a large pool, upon transmitting 100 LFM signals with $W_0 = 8$ kHz centered at 20 kHz, $T_0 = 50$ ms, and $f_s = 100$ kHz. In Fig. 2, we plot the ROC curves when the two hydrophones are jointly used as a detector with $K = 2$ sensors. The improved performance of this detector is noticeable, with SNR of 12.4 dB, compared to the single-sensor detectors that use only hydrophone B or A, with SNRs of 10.1 and 8.1 dB, respectively. The multi-sensor performance improvement demonstrated using measured data agrees with the similar observation made using simulations in the previous section.

V. CONCLUSION

In this paper, we have derived and studied a multi-sensor detector for time-spreading distortion (TSD) underwater channels that have multiple propagation paths. The detector is optimal under certain assumptions mentioned in the paper. We have also assessed the performance of the detector using both Monte Carlo simulations and experimental underwater data. Our results indicate that, as the number of sensors increases, the performance of the detector improves. This can be attributed to the SNR increase. We have also quantified how the number of correlators per sensor can affect the performance. Further studies are underway to understand other aspects of signal detection in underwater TSD channels.

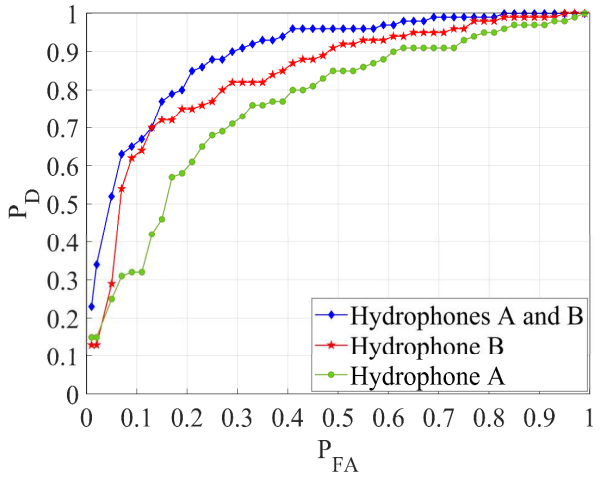

Fig. 2. Experimental ROC curve using two hydrophones jointly with $M = 20$, versus individual experimental ROC curves when each hydrophone is individually used for signal detection.

REFERENCES

[1] P. Baggenstoss, "On detecting linear frequency modulated waveforms in frequency- and time-dispersive channels: Alternatives to segmented replica correlation," *IEEE J. Oceanic Engineering,* vol. 19, pp. 591- 598, 1994.

[2] B. Friedlander and A. Zeira, "Detection of broadband signals in frequency and time dispersive channels," *IEEE Trans. Signal Processing*, vol. 44, pp. 1613-1622, 1996.

[3] Z.-H. Michalopoulou, "Active source detection in a dispersive multiple-reflection environment," in *Proc. IEEE Int. Conf. Acoust., Speech, Signal Processing*, Phoenix, AZ, 1999, pp. 2765-2768.

[4] R. Rashid, E. Zhang, Z.-H. Michalopoulou and A. Abdi, "Signal detection in time spreading underwater environments using vector and scalar sensors," presented at the *181st Meet. Acoust. Soc. Am.,* Seattle, WA, 2021.

[5] X. Pan, Z. Liu, P. Zhang, Y. Shen and J. Qiu "Distributed MIMO sonar for detection of moving targets in shallow sea environments," *Applied Acoustics*, vol. 185, 108366, 2022.

[6] Z.-H. Michalopoulou, A. Pole and A. Abdi, "Bayesian coherent and incoherent matched-field localization and detection in the ocean," *J. Acoust. Soc. Am.*, vol. 146, pp. 4812–4820, 2019.

[7] S. M. Kay, *Fundamentals of Statistical Signal Processing: Estimation Theory*. Prentice-Hall, 1993.

[8] S .M. Kay, *Fundamentals of Statistical Signal Processing: Detection Theory*. Prentice-Hall, 1998.